Journal of Catalysis **205,** 382–387 (2002)
doi:10.1006/jcat.2001.3442, available online at http://www.idealibrary.com on IDEAL®

Optimal Catalyst Curves: Connecting Density Functional Theory Calculations with Industrial Reactor Design and Catalyst Selection

Claus J. H. Jacobsen,*[,1] Søren Dahl,* Astrid Boisen,* Bjerne S. Clausen,* Henrik Topsøe,*
Ashildur Logadottir,† and Jens K. Nørskov†

*Haldor Topsøe A/S, Nymøllevej 55, DK-2800 Lyngby, Denmark; and †Center for Atomic-Scale Materials Physics (CAMP),
Technical University of Denmark, DK-2800 Lyngby, Denmark*

Received August 14, 2001; revised September 27, 2001; accepted September 27, 2001; published online January 3, 2002

For ammonia synthesis catalysts a volcano-type relationship has been found experimentally. We demonstrate that by combining density functional theory calculations with a microkinetic model the position of the maximum of the volcano curve is sensitive to the reaction conditions. The catalytic ammonia synthesis activity, to a first approximation, is a function only of the binding energy of nitrogen to the catalyst. Therefore, it is possible to evaluate which nitrogen binding energy is optimal under given reaction conditions. This leads to the concept of optimal catalyst curves, which illustrate the nitrogen binding energies of the optimal catalysts at different temperatures, pressures, and synthesis gas compositions. Using this concept together with the ability to prepare catalysts with desired binding energies it is possible to optimize the ammonia process. In this way a link between first-principle quantum mechanical calculations of gas–surface interactions, reactor design, and catalyst selection has been established for the first time.

Key Words: **ammonia synthesis; volcano curve; microkinetic model; density functional theory; optimal catalyst curves; reactor design; catalyst selection.**

INTRODUCTION

For several heterogeneous catalytic reactions, the activities of different transition metal catalysts are described by a Sabatier-type relationship (1). This variation of the catalytic activity with the position of the transition metal in the Periodic Table is usually expressed as a volcano curve as first proposed by Balandin (2). For ammonia synthesis catalysts such a volcano curve has been found experimentally (3) as shown in Fig. 1.

Recently, we have shown that this activity trend can be accurately rationalized by combining the results of density functional theory (DFT) calculations (4) with a microkinetic model for ammonia synthesis (5) that takes the electronic promotion into account (6). The predictions from this model can also be seen in Fig. 1. It is apparent that even though the model is a first approximation that does not take small local variations into consideration, it captures the reactivity trends very well, particularly for catalysts in the industrially relevant region. It should also be noted that the experimental results are subject to significant uncertainty due both to the large activity differences between the catalysts and to the difficulty related to counting the number of active sites. Particularly, the latter can be huge due to the severe structure sensitivity of ammonia synthesis observed in surface science studies (7–9), catalyst studies (5, 10, 11), and DFT modeling (4, 12, 13).

In our model (4), ammonia synthesis kinetics is determined solely by the binding energy of nitrogen to the surface, and the most active catalysts are characterized by a nitrogen binding energy of intermediate size. Recently, we have shown how the published activities of the bimetallic ammonia synthesis catalyst can also be rationalized with this model (14) and that new active catalysts can be designed by combining metals with nitrogen binding energies higher and lower than the optimum (15–17). Volcano curves have been observed for several other catalytic reactions. The classical example is formate decomposition (1), but also for other reactions of significant interest, such as Fischer–Tropsch synthesis (18) and hydrotreating (19, 20), such a relationship has been found.

For hydrotreating catalysts it is known that the relative catalytic activities of different catalysts are dependent on the reaction conditions, particularly the H_2S partial pressure (20). For ammonia synthesis catalysts it has also been verified experimentally that the activity trends are influenced by the reaction conditions. For example, it is usually found that promoted iron catalysts are better than promoted ruthenium catalysts at low ammonia concentrations, whereas the opposite situation is found at high ammonia concentrations (21). However, thus far, this influence of the reaction conditions on the volcano curve has not been quantified for any heterogeneous catalytic reaction. Our model (4, 6) for the ammonia synthesis reaction describes the reaction kinetics of promoted transition metal catalysts

---

[1] To whom correspondence should be addressed. Fax: 45 45 27 29 99. E-mail: chj@topsoe.dk.

0021-9517/02 $35.00

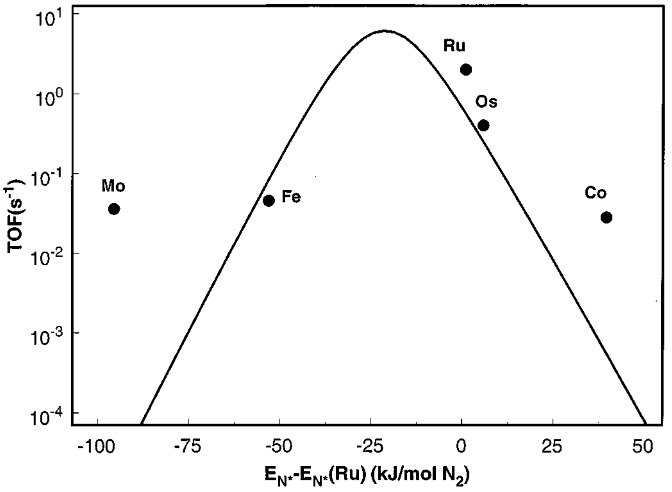

FIG. 1. Volcano curve for promoted ammonia synthesis catalysts showing the turnover frequency for different nitrogen binding energies. Experimental results are extracted from Aika and Tamaru (3) assuming that 1% of the metal surface sites is active for dissociation of dinitrogen and all catalysts have the same amount of active sites. The volcano curve (full line) is calculated assuming conditions as close to the experiments as possible: 0.8 bar, 588 K, $H_2 : N_2 = 3$, 0.1%NH_3.

well, and therefore such effects can now be studied. Since the catalytic ammonia synthesis activity is dependent only on the nitrogen binding energy, it is possible to establish which nitrogen binding energy is optimal under given reaction conditions. This leads to the concept of optimal catalyst curves, which illustrate the nitrogen binding energies of the optimal catalysts at different temperatures, pressures, and synthesis gas compositions. By comparing the optimal catalyst curves with the operating line that connects the temperature and ammonia concentrations in the catalytic reactor during operation, we show how it is possible to choose or design the optimal catalyst(s). The smallest possible catalytic reactor can be designed when both the optimum catalyst curves and the optimum operating line are taken into account. In this way it is possible for the first time to link first-principle quantum mechanical calculations of gas–surface interactions with reactor design and catalyst selection.

We illustrate the procedure for ammonia synthesis for which we have accurate rate expressions. However, a similar approach should also be possible for other reactions when sufficient insight becomes available.

METHODS

Calculation of Volcano Curves

The procedure for calculating the volcano curves has been described in detail elsewhere (6). The turnover frequency (TOF) under a given set of synthesis conditions is determined through the microkinetic model by the activation energy for dinitrogen dissociation and the binding energies of the different surface intermediates involved in ammonia synthesis. Figure 2 illustrates how we relate these energies to the nitrogen binding energy. This enables a first approximation of the TOF as a function of only one parameter, the nitrogen binding energy, to be established.

In Fig. 2 the surface binding energies are given as potential energies per two nitrogen atoms. Throughout this paper the nitrogen binding energies are represented in the same way. In the volcano curves, we have included some of the elements for which accurate nitrogen binding energies have been calculated. In general, the nitrogen binding energy varies monotonically through the periods of the Periodic Table, so it is simple to estimate the nitrogen binding energies of other metals. Consequently, the volcano curves are shown as TOF vs nitrogen binding energies relative to that on ruthenium. In practice, the relevant catalytic activity is the turnover frequency multiplied by the density of sites, e.g., the number of sites for a given mass or the number of sites for a given volume of catalyst. Therefore, the benefits of a high TOF can only be realized if a sufficiently high density of sites can be achieved. Industrially, the cost of a given number of active sites is an equally important parameter.

Calculation of Equilibrium Curves

The equilibrium curves as a function of temperature, pressure, and gas composition are calculated using the routines of Kjær and Christiansen (22, 23).

Calculation of Optimal Operating (Maximum Rate) Lines

The optimal operating lines are shown as curves parallel to the equilibrium curve. In practice they are for industrially relevant conditions, usually shifted between 30 and 60°C from the equilibrium line. However, for our purposes the curves shown give a sufficiently accurate estimate of the optimal operating line for the relevant reaction conditions (24). It should be noted that the optimal operating line will have a slightly different position for every catalyst. If desired, the accurate position of the optimal operating

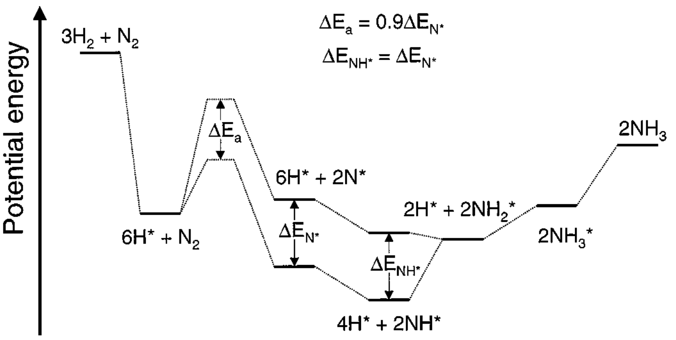

FIG. 2. Energy level diagram for catalytic ammonia synthesis used for calculation of volcano curve. It is shown how the energies relevant for ammonia synthesis change when the binding energy of nitrogen is changed.

line can be found by setting $dr/dT = 0$, where r is the rate expression given as a function of $p(NH_3)$ and T.

Calculation of Optimal Catalyst Curves

From the volcano curves calculated, as described earlier, the optimal catalyst curves can be constructed. For a given total pressure and $H_2 : N_2$ ratio this can be done by calculation of volcano curves for different temperatures and ammonia concentrations. For each set of reaction conditions the nitrogen binding energy corresponding to the maximum of the volcano curve is plotted in a diagram showing ammonia concentration vs temperature. By connecting data points representing the same binding energies, the optimal catalyst curves are obtained, e.g., curves showing under which conditions a catalyst with given nitrogen binding energy is optimal.

RESULTS AND DISCUSSION

Figure 3 shows how the maximum of the volcano curve is shifted as the ammonia concentration is increased. In both diagrams, the volcano curves are calculated at ammonia concentrations representing a 5, 20, and 90% approach to equilibrium. It is seen that at 420°C with a $H_2 : N_2$ ratio of 2 : 1 and at the relatively low pressure (80 bar) as seen in the left panel of Fig. 3, the optimal catalyst at high ammonia concentrations has a nitrogen binding energy close to that of ruthenium, whereas at the lowest ammonia concentrations a nitrogen binding energy closer to that of iron is optimal.

The right panel of Fig. 3 shows similarly how the volcano curve is shifted when the ammonia concentration varies. These volcano curves are calculated at 450°C and 200 bar with a $H_2 : N_2$ ratio of 3 : 1, and the optimal catalysts have binding energies relatively closest to those of iron, except at the highest ammonia concentrations. These trends are in agreement with experimental findings. Previously, we have shown how the model accurately describes not only the effect of electronic promotion (6) but also the alloying effects (14). It is now possible to understand many of the apparently conflicting experimental observations reported for ammonia synthesis catalysts, since the effects of promotion and alloying depend critically on the experimental conditions. For example, many different views on the effect of Co addition to the traditional promoted iron catalyst have been presented (25–27). However, promoted Fe–Co catalysts are only expected to be better than promoted Fe catalysts at relatively high ammonia concentrations. This is due to the lower ammonia inhibition of such catalysts compared to that of promoted iron catalysts. In this sense the properties of promoted Fe–Co catalysts are intermediate between those of promoted iron and cobalt in accordance with the interpolation principle (14). Generally, it should be noted that the proper use of the interpolation concept requires knowledge of the catalyst surface composition under the relevant reaction conditions.

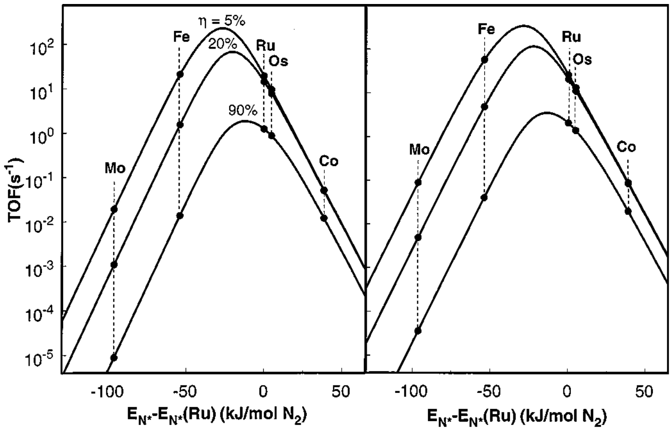

FIG. 3. (Left panel): Calculated volcano curves at 420°C, 80 bar, 2 : 1 $H_2 : N_2$, equilibrium 17.4% NH_3. (Right panel): Calculated volcano curves at 450°C, 200 bar, 3 : 1 $H_2 : N_2$; equilibrium 25.4% NH_3. In both cases the volcano curves are calculated at ammonia concentrations corresponding to a 90, 20, and 5% approach to equilibrium.

Ammonia synthesis is an equilibrium-limited exothermic reaction. This is also the case for many other large-scale catalytic reactions of industrial interest such as methanol synthesis, water–gas shift, benzene hydrogenation, and sulfur dioxide oxidation. If the heat of reaction is not removed, the ammonia concentration and the temperature will increase until equilibrium is established.

As a starting point we consider ammonia synthesis in an isothermal reactor at atmospheric pressure. Figure 4 shows the position of the equilibrium curve under these conditions. Since the reaction is exothermic, the equilibrium concentration of ammonia decreases when the temperature increases. In laboratory reactors, ammonia synthesis is often conducted at atmospheric pressure and at a temperature around 350°C. Usually, it is not a problem to achieve isothermal operation under these conditions due to the very small conversion. Figure 4 illustrates the operating line that connects the temperature and the ammonia concentration in such a reactor.

Since it is an isothermal reactor the operating line is vertical. For example, the ammonia concentration increases from 0.01 to 0.80% in the experiment as illustrated by the starting and ending points of the operating line. We have shown that the position of the maximum of the volcano curve depends on the reaction conditions. Therefore, to minimize the amount of catalyst required to reach the given ammonia concentration, it is possible that different catalysts should be chosen for the different reaction conditions (in this case for the different ammonia concentrations), and this is indeed the case. To determine which catalysts should optimally be chosen, we have included some optimal catalyst curves in Fig. 4. In principle, an infinite number of

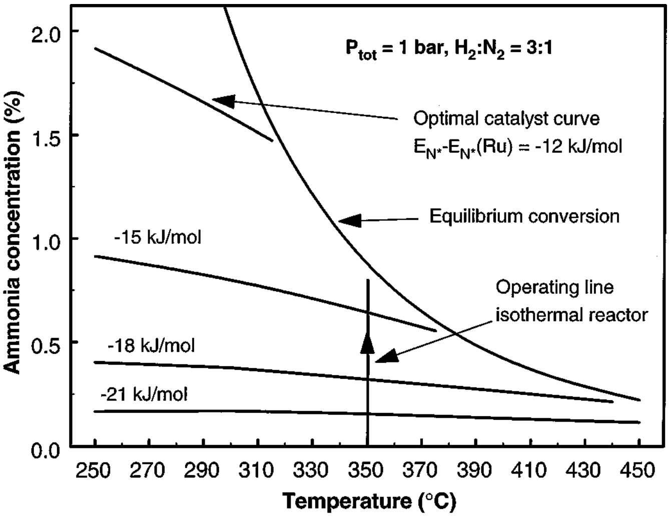

FIG. 4. Equilibrium curve at atmospheric pressure and operating line for an isothermal reactor operating at 350°C in which the ammonia concentration is increased from 0.01 to 0.80%. The optimal catalyst curves intersect the operating line. This shows that different catalysts are optimal for the different reaction conditions in the reactor.

optimal catalyst curves corresponding to different nitrogen binding energies exist. These curves show the binding energy of nitrogen for the catalyst with the highest turnover frequency under the given conditions. The optimal catalyst curves are seen to pass through the operating line. At the inlet of the reactor, a nitrogen binding energy, E_{N*}–E_{N*}(Ru), of about −30 kJ/mol is optimal, whereas −13 kJ/mol is optimal at the outlet. This means that the minimal amount of catalyst is necessary if an infinite number of different catalysts with carefully chosen nitrogen binding energies are used. Each catalyst must be placed in the reactor so that it experiences the reaction conditions defined by the intersection of the relevant optimal catalyst curve and the operating line. In practice, it is of course not possible to select an infinite number of catalysts with the desired nitrogen binding energies. Furthermore, it is not possible to operate an industrial reactor isothermally. For ammonia synthesis, the adiabatic temperature rise is ca. 14–18°C for each percentage of ammonia produced (28, 29). Therefore, only a quite small conversion per pass can be reached in the ammonia synthesis loop. Using only a single catalyst, it is well known that the minimum catalyst volume will be obtained in a reactor where the optimal operating line is followed as closely as possible. The optimal operating line, occasionally also called the maximum rate line, illustrates the temperatures at which the maximum rate is reached at given pressure and gas composition. Different synthesis loop configurations have been proposed to approximate the optimal operating line. Figure 5 shows how it is done in an internally cooled reactor with a countercurrent flow of synthesis gas in the cooling tubes or in an indirectly cooled reactor where the gas is cooled by heat exchange between the individual beds. The resulting operating lines are also shown (30). These two reactor designs have been extensively used in the ammonia synthesis industry. The TVA reactor that was common from 1930 to 1965 typifies the internally cooled reactor. Today, most new industrial ammonia synthesis reactors are adiabatic two- or three-bed radial flow arrangements with indirect cooling. In such reactors, the ammonia concentration and the temperature vary in the two (or three) beds as shown in Fig. 5.

As was the case for the isothermal reactor, it is possible that different catalysts should be chosen for the two (or three) catalyst beds in the indirectly cooled reactor to minimize the total catalyst volume. Again, this can easily be seen by including some optimal catalyst curves with the operating line. In Fig. 6, we have done this for a three-bed arrangement with indirect cooling in a synthesis loop at 200 bar with a stoichiometric synthesis gas.

Similarly, optimal catalyst curves are shown at a synthesis pressure of 80 bar with a H_2 : N_2 ratio of 2 : 1. In the high

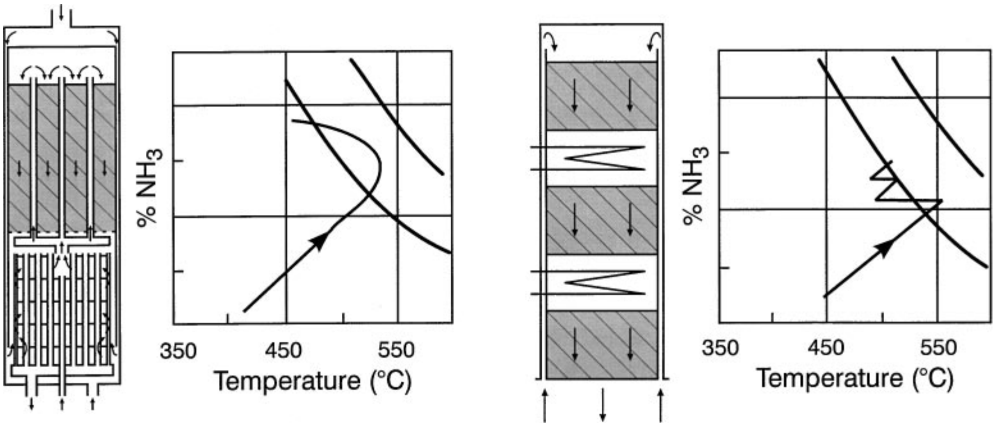

FIG. 5. $p(NH_3)$ vs T diagrams illustrating the equilibrium curve and the operating line for an internally cooled reactor (left). An indirectly cooled reactor with three beds (right).

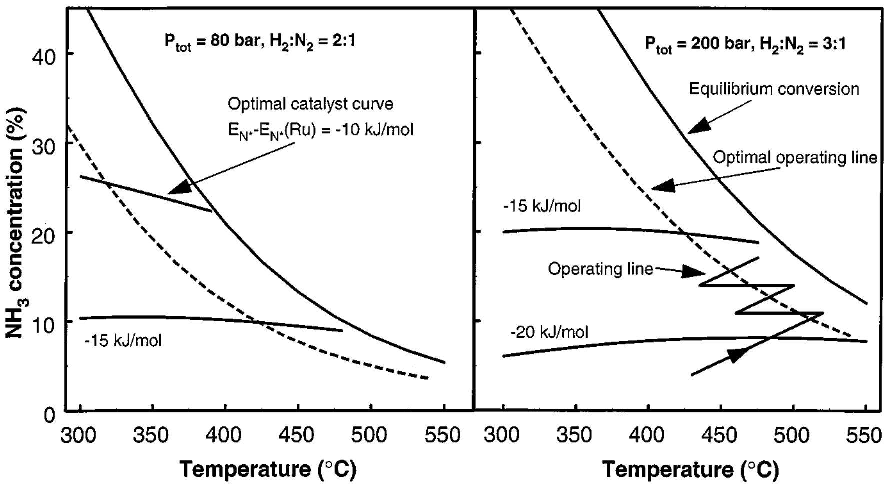

FIG. 6. Optimal catalyst curves superimposed on a $p(NH_3)$ vs T diagram with equilibrium curve and optimal operating line for an indirectly cooled reactor with three beds with an $H_2 : N_2$ ratio of 3 : 1 at 200 bar (right). Two beds with an $H_2 : N_2$ ratio of 2 : 1 at 80 bar (left).

pressure case, it is seen that catalysts with nitrogen binding energies, E_{N^*}–E_{N^*}(Ru), between −15 and −25 kJ/mol are optimal dependent on the position in the reactor. If a similar operating line is drawn for the low pressure case, it is apparent that catalysts with binding energies between −10 and −20 kJ/mol are optimal. In all cases it is seen that the optimal catalyst curves cross the optimal operating line. Thus, it is seen that the smallest possible amount of catalyst is necessary when an infinite number of different catalysts are used in all three beds. For each bed the situation is analogous to the case of the isothermal reactor. Although it is not possible to use an infinte number of catalysts in each bed, it could easily be possible to use different catalysts in the three beds. In such a case, it is desirable to select catalysts with nitrogen binding energies, E_{N^*}–E_{N^*}(Ru) close to those corresponding to the intersections of the optimal catalyst curves and the operating line. Generally however, the smallest possible total catalyst volume results when the reactor is designed to follow the optimal operating line as closely as possible, and simultaneously the catalysts are selected to approach the optimal catalyst curves as closely as possible. It is a simple optimization to balance the potential savings in the reactor volume against the cost of available catalysts. It is worth noting that the considerations presented here are in excellent agreement with industrial practice. In ammonia synthesis loops operated at high pressures only iron catalysts are used, whereas ruthenium catalysts are used in the second, third, and fourth bed of the Kellogg advanced ammonia process (31, 32) operated at lower pressure and with a $H_2 : N_2$ ratio below 3 and close to equilibrium.

This means that with our current understanding of the ammonia synthesis reaction it is possible to link density functional calculations with the industrial reactor design and catalyst selection. Thus far, this is only possible in ammonia synthesis due to the in-depth understanding of this reaction. For other reactions we anticipate that a similar situation will be reached when more detailed models become available. However, ammonia synthesis represents a rather simple case since the activity can be accurately described by a single parameter. For other reactions this might not be possible. However, it should still be possible to establish optimal catalyst curves, although they might not be easily visualized.

REFERENCES

1. Sabatier, P., "La Catalyse en Chimie Organique." Bérange, Paris, 1920.
2. Balandin, A. A., *Adv. Catal.* **19**, 1 (1969).
3. Aika, K., and Tamaru, K., *in* "Ammonia: Catalysis and Manufacture" (A. Nielsen, Ed.), p. 103. Springer-Verlag, Berlin/Heidelberg, 1995.
4. Logadottir, A., Rod, T. H., Nørskov, J. K., Hammer, B., Dahl, S., and Jacobsen, C. J. H., *J. Catal.* **197**, 229 (2001).
5. Dahl, S., Sehested, J., Jacobsen, C. J. H., Törnqvist, E., and Chorkendorff, I., *J. Catal.* **192**, 391 (2000).
6. Dahl, S., Logadottir, A., Jacobsen, C. J. H., and Nørskov, J. K., *Appl. Catal.* in press.
7. Ertl, G., *in* "Catalytic Ammonia Synthesis" (J. R. Jennings, Ed.), p. 109. Plenum, New York, 1991.
8. Materer, N., and Somorjai, G. A., *Topics Catal.* **1**, 215 (1994).
9. Dahl, S., Törnqvist, E., and Chorkendorff, I., *J. Catal.* **192**, 391 (2000).
10. Dumesic, J. A., Topsøe, H., Khammouma, S., and Boudart, M., *J. Catal.* **37**, 503 (1975).
11. Dahl, S., Törnqvist, E., and Jacobsen, C. J. H., *J. Catal.* **198**, 97 (2000).
12. Dahl, S., Logadottir, A., Egeberg, R. C., Larsen, J. H., Chorkendorff, I., Törnqvist, E., and Nørskov, J. K., *Phys. Rev. Lett.* **83**, 1814 (1999).
13. Mortensen, J. J., Hansen, L. B., Hammer, B., and Nørskov, J. K., *J. Catal.* **182**, 479 (1999).
14. Jacobsen, C. J. H., Dahl, S., Clausen, B. S., Bahn, S., Logadottir, A., and Nørskov, J. K., *J. Am. Chem. Soc.* **123**, 8404 (2001).
15. Jacobsen, C. J. H., *Chem. Commun.* 1057 (2000).
16. Jacobsen, C. J. H., Brorson, M., Sehested, J., Teunissen, H., and Törnqvist, E., U.S. Patent 6,235,676 (assigned to Haldor Topsøe A/S) (1999).
17. Kojima, R., and Aika, K., *Chem. Lett.* 514 (2000).
18. Vannice, M. A., *J. Catal.* **50**, 228 (1977).

19. Pecoraro, T. A., and Chianelli, R. R., *J. Catal.* **67**, 432 (1981).
20. Topsøe, H., Clausen, B. S., Massoth, "Catalysis Science and Technology" (J. R. Anderson and M. Boudart, Eds.), Vol. 11. Springer-Verlag, Berlin, 1996.
21. Tennison, S. R., *in* "Catalytic Ammonia Synthesis" (J. R. Jennings, Ed.), p. 303. Plenum, New York, 1991.
22. Christiansen, L. J., and Kjær, J., "Enthalpy Tables of Ideal Gasses." Haldor Topsøe A/S, Copenhagen, 1982.
23. Christiansen, L. J., *in* "Ammonia: Catalysis and Manufacture" (A. Nielsen, Ed.), p. 1. Springer-Verlag, Berlin/Heidenberg, 1995.
24. Dybkjær, I., *in* "Ammonia: Catalysis and Manufacture" (A. Nielsen, Ed.), p. 199. Springer-Verlag, Berlin/Heidelberg, 1995.
25. Artyuk, Y. N., Rusov, M. T., and Boldyreva, N. A., *Kinet. Katal.* **8**, 114 (1967).
26. Taylor, D. W., Smith, P. J., Dowden, D. A., Kemball, C., and Whan, D. A., *Appl. Catal.* **3**, 161 (1982).
27. Jennings, J. R., U.S. Patent 4,668,657 (assigned to ICI) (1987).
28. Gramatica, G., and Pernicone, N., *in* "Catalytic Ammonia Synthesis" (J. R. Jennings, Ed.), p. 211. Plenum, New York, 1991.
29. Appl, M., "Ullmann's Encyclopedia of Industrial Chemistry," 6 th edition. VCH Verlag, Weinheim, 2000.
30. Fodor, L., *Chim. Ind. Genie. Chim.* **104**, 1002 (1971).
31. Czuppon, T. A., Knez, S. A., Schneider, R. W., and Worobets, G., *Ammonia Plant Safety Relat. Facil.* **34**, 236 (1994).
32. Strait, R., *Nitrog. Methan.* **238**, 37 (1999).